

VEHICLE DISPATCHING IN MODULAR TRANSIT NETWORKS: A NONLINEAR MIXED-INTEGER PROGRAMMING MODEL

Mingyang Pei^{1,3}, Peiqun Lin¹, Jun Du^{2,3}, Xiaopeng Li^{3*}, and Zhiwei Chen³

¹ *Department of Civil and Transportation Engineering, South China University of Technology, Guangzhou 510641, China, Mingyang Pei email: ratherthan@foxmail.com and Peiqun Lin pqlin@scut.edu.cn*

² *MOE Key Laboratory for Urban Transportation Complex Systems Theory and Technology, Beijing Jiaotong University, Beijing 100044, China, Jun Du email: 16114234@bjtu.edu.cn*

³ *Department of Civil and Environmental Engineering, University of South Florida, FL 33620, USA, *Corresponding author Xiaopeng (Shaw) Li, email: xiaopengli@usf.edu and Zhiwei Chen email: zhiweic@usf.edu*

ABSTRACT

Modular vehicle (MV) technology offers the possibility of flexibly adjusting the vehicle capacity by docking/undocking modular pods into vehicles of different sizes en route to satisfy passenger demand. Based on the MV technology, a modular transit network system (MTNS) concept is proposed to overcome the mismatch between fixed vehicle capacity and spatially varying travel demand in traditional public transportation systems. To achieve the optimal MTNS design, a mixed-integer nonlinear programming model is developed to balance the tradeoff between the vehicle operation cost and the passenger trip time cost. The nonlinear model is reformulated into a computationally tractable linear model. The linear model solves the lower and upper bounds of the original nonlinear model to produce a near-optimal solution to the MTNS design. This reformulated linear model can be solved with off-the-shelf commercial solvers (e.g., Gurobi). Two numerical examples in different contexts are used to demonstrate the applicability of the proposed model and its effectiveness in reducing system costs.

Keywords: public transit; modular vehicle; operation design; mixed-integer nonlinear programming

³ Corresponding author. Tel: +1-813-974-0778; Email: xiaopengli@usf.edu.

VEHICLE DISPATCHING IN MODULAR TRANSIT NETWORKS: A NONLINEAR MIXED-INTEGER PROGRAMMING MODEL

ABSTRACT

Modular vehicle (MV) technology offers the possibility of flexibly adjusting the vehicle capacity by docking/undocking modular pods into vehicles of different sizes en route to satisfy passenger demand. Based on the MV technology, a modular transit network system (MTNS) concept is proposed to overcome the mismatch between fixed vehicle capacity and spatially varying travel demand in traditional public transportation systems. To achieve the optimal MTNS design, a mixed-integer nonlinear programming model is developed to balance the tradeoff between the vehicle operation cost and the passenger trip time cost. The nonlinear model is reformulated into a computationally tractable linear model. The linear model solves the lower and upper bounds of the original nonlinear model to produce a near-optimal solution to the MTNS design. This reformulated linear model can be solved with off-the-shelf commercial solvers (e.g., Gurobi). Two numerical examples in different contexts are used to demonstrate the applicability of the proposed model and its effectiveness in reducing system costs.

Keywords: public transit; modular vehicle; operational design; mixed-integer nonlinear programming

1. Introduction

Most current public transportation systems (e.g., mass transit) adopt vehicles with fixed capacities that cannot adapt to the temporal and spatial variations in travel demand. This mismatch between vehicle capacity and travel demand causes either excessive passenger waiting (e.g., in areas with a high demand relative to the vehicle capacity) or low vehicle occupancy (e.g., in areas with a high vehicle capacity relative to the demand).

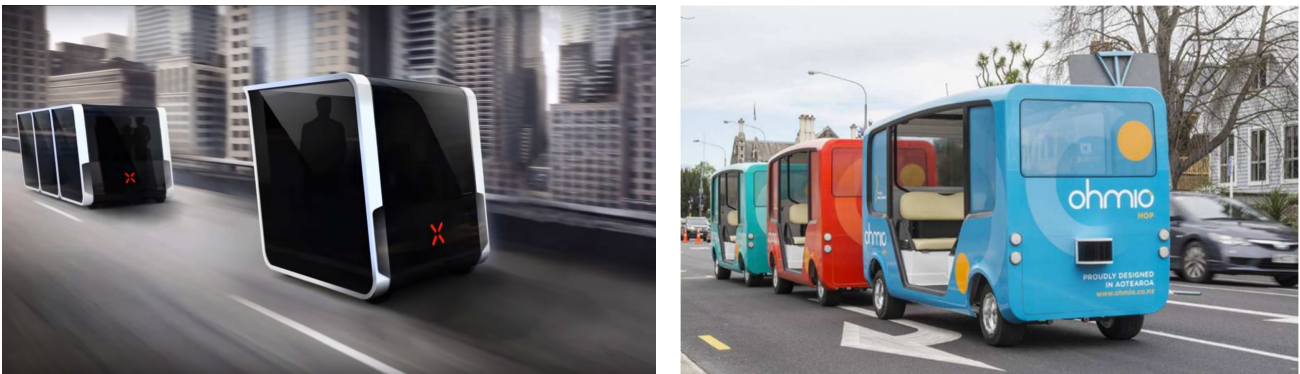


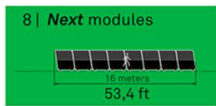
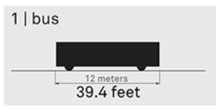
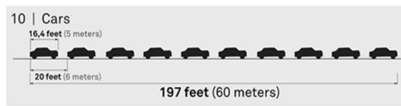
Figure 1 MV concepts proposed by (a) NEXT (source: <https://www.next-future-mobility.com>) and (b) Ohmio LIFT (source: <https://ohmio.com>).

Emerging modular vehicle (MV) technology holds the promise of overcoming these issues. The MV technology allows modular pods to be dynamically docked/undocked into vehicles of different sizes en route (Figure 1; Chen et al., 2019, 2020). This technology have been tested by multiple companies, such as NEXT (Next Future Transport, 2019) and Ohmio LIFT (Ohmio, 2018). We propose a modular transit network system (MTNS) that uses the MV technology. In the MTNS system, MVs that operate in a transportation network can be quickly reassembled at nodes (or stations) to obtain different capacities that suit the downstream travel demand. With flexible vehicle capacity adjustment, the MTNS can

effectively reduce the passenger waiting time (by forming long MV chains) and improve the vehicle occupancy (by forming short MV chains) to overcome the limitations of traditional public transportation systems. According to the economies of scale in urban mass transportation, the travel cost of a vehicle is usually a concave function of the number of modular pods in it (Chen et al., 2020). As a result, this MTNS has potentials in reducing the system operation cost.

We aim to optimally allocate and schedule an MV fleet over a general transportation network to achieve the optimal balance between operating cost and passenger trip time cost. Decisions include the dispatch frequency and vehicle capacity for each dispatch. To better verify the utility of the MTNS, we compare it with two benchmark systems: the fixed-capacity shuttle bus system (FSBS) and the passenger car system (PCS). The FSBS can be considered a special case of the MTNS, where each vehicle has a fixed capacity and provides transportation service without intermediate stops. The FSBS is used mostly in areas where bus stops are sparse and scattered; in these areas, there is a low economic incentive for intermediate stops because of the long detour distance. Since the capacities of the vehicles are fixed, the performance of the FSBS may be limited if the passenger demand exhibits considerable spatial variation. Specifically, the FSBS may not fully utilize the vehicle capacity in places with low demand, and it may not be able to serve all passengers in places with intensive demand. In contrast, the vehicle capacity in a general MTNS is adjustable to passenger demand. Therefore, the MTNS better fits varying passenger demand by dynamically adjusting the vehicle capacity. Further, vehicles in a PCS are private passenger cars (or taxis) with a small fixed capacity. The advantage of a PCS is service convenience for individual travelers (e.g., direct door-to-door service and no waiting and transfer times). However, a PCS may be the most expensive system, since more vehicles are required to serve the same demand. A detailed comparison of the three systems is provided in Table 1.

Table 1 Comparison of alternative systems

	MTNS	FSBS	PCS
Overall cost	Operation cost; Waiting time cost; Riding time cost	Operation cost; Waiting time cost; Riding time cost	Operation cost; Riding time cost
Transfer cost	Considered	Considered	No
Transfer mode	Walk	In-vehicle transferred	No
Vehicle type	Flexible capacity	Fixed capacity	Fixed capacity
Occupancy	6 passengers/pod	36~48 passengers/bus	1~4 passengers/car
Vehicle length (48 passengers)	 Flexible; small per passenger	 Fixed; small per passenger	 Fixed; long per passenger

Note: Data and figure source: <https://www.next-future-mobility.com>

A class of related studies has focused on designing a transit system to serve a transportation network. However, few studies have investigated the design of MTNSs in the literature. Most current studies have focused on transportation network design to provide comprehensive services to an urban area (Almasi et al., 2018; Cepeda et al., 2006; Daganzo, 2010; Fan et al., 2018; Guo et al., 2017; Nourbakhsh and Ouyang, 2012; Tong and Wong, 1999; Wu et al., 2016). The goal is to minimize the

1 total system cost, which includes the operation costs (Alshalalfah and Shalaby, 2012; Diana et al., 2006;
2 Nourbakhsh and Ouyang, 2012; Pei et al., 2019a; Quadrifoglio et al., 2006, 2007, 2008), trip time costs
3 (Niu et al., 2015; Pei et al., 2019b; Quadrifoglio et al., 2008), accessibility (Nassir et al., 2016; Owen
4 and Levinson, 2015), etc. For example, Ortega and Wolsey (2003) investigated an incapacitated fixed-
5 charge network flow problem to minimize the network design costs and passenger flow costs. Daganzo
6 (2010) analyzed the structure of urban transit networks to increase accessibility. Ouyang et al. (2014)
7 used the continuum approximation technique to design bus networks for cities where the travel demand
8 gradually varies in space. The authors proposed heterogeneous route configurations to reduce the costs
9 for both bus users and the operating agency. Tong et al. (2015) developed an urban transit network
10 design model to maximize the number of accessible activity locations in a space-time network within a
11 given travel time budget. Despite these fruitful developments, most existing transit network design
12 studies have only considered vehicles with fixed capacity.

13 Few recent studies have investigated MV operations in transit systems. Table 2 briefly summarizes
14 these studies. Most of these studies propose a variable-capacity operation approach with modular transits
15 based on the MV concept. Guo et al. (2018) proposed a simulation-based model to design a many-to-one
16 (M-to-1) system in the MV context. (Chen et al., 2019, 2020) proposed both discrete and continuous
17 models to design an MV shuttle system under oversaturated traffic conditions. Rau et al. (2019)
18 proposed a dynamic autonomous road transit system by varying the number of modular pods in each
19 vehicle. Zhang et al.(2020) mathematically modeled an MV transit system with a time-expanded
20 network to reduce the size of the optimization problem. Shi et al. (2020) proposed a variable-capacity
21 operation approach for two corridors that shared a portion of stations. Caros and Chow (2020) proposed
22 a two-sided day-to-day learning framework to simulate the performance of a mobility service using
23 modular autonomous vehicles capable of en-route passenger transfers. Dai et al., (2020) proposed a joint
24 design of bus capacity and dispatch headway in a mixed traffic environment that consisted of both
25 human-driven vehicles and MVs. Despite these pioneering explorations, most studies have only
26 considered a shuttle system or a transit line, and vehicle dispatching for the proposed MTNS has not
27 been well studied. Although one may be easily tempted by the idea of solving the MTNS design with
28 existing methods because we only must jointly design the service frequency and capacity of each shuttle
29 route, the problem under investigation is much more complicated for two reasons. First, a network
30 consists of multiple lines, so there are interactions among different lines (e.g., transfer). These
31 interactions are not modeled in transit line/shuttle studies, so the existing methods cannot be directly
32 used. Second, the problem of designing one transit line is NP-hard (Liu and Ceder, 2017; Sayarshad and
33 Chow, 2015; Wang and Qu, 2015), so most studies have simply proposed heuristics to solve near-
34 optimal solutions. A network model is a harder NP-hard problem due to many more decision variables
35 (since there are more lines and transfer decisions) and constraints (since we must add constraints to
36 describe the interactions of different lines). Thus, most existing solution algorithms for transit network
37 designs likely fail due to the dramatic increase in solution space.

38 **Table 2 Comparison of the current related models and the proposed model**

Paper	Objective function	Decision variable(s)	Model type*	Constraint type	Vehicle type	Vehicle rebalance	System topology	Model approach
Niu et al. (2015)	Passenger waiting time	Timetable, dwelling time, and speed profile	MINLP	Linear constraints	Fixed-capacity vehicle	No	Corridor	Mathematical programming

Chen et al., (2020, 2019)	Operation cost; passenger waiting time	Timetable and vehicle types	MILP & CA	Linear constraints	MV	No	Shuttle	Mathematical programming & analytical model
Guo et al. (2018)	Myopic policy cost	Switching of transit service	-	Linear constraints	MV	No	M-to-1 network	Simulation
Rau et al.,(2019)	Effective use of capacity	Adaptive Fleet Size	-	-	MV	No	Network	Simulation
Caros and Chow(2020)	operator cost and user cost	En-route transfer	MILP	-	MV	No	Hub-and-spoke	Simulation/insertion heuristic
Zhang et al.(2020)	Number of served requests	Timetable; vehicle types; module match	MILP	Linear constraints	MV	No	Network	Mathematical programming
Shi et al. (2020)	Operation cost; passenger waiting time	Timetable; vehicle types	MILP	Nonlinear constraints	MV	No	Corridor	Mathematical programming
Dai et al., (2020)	Operation costs; waiting time	scheduling and capacity	MINLP	Linear constraints	MV	No	Corridor	Mathematical programming
Our model	Operation cost; total time cost	Transfer strategies; vehicle types	MINLP	Linear constraints	MV	Considered	Network	Mathematical programming

Note: MINLP=mixed-integer nonlinear programming; MILP=mixed-integer linear programming; CA=continuum approximation

To bridge these gaps and achieve the vision of MTNSs, this paper proposes a mathematical approach to describe MTNS operations and determine the optimal MTNS design. The contributions of this paper are as follows.

First, previous works predominately focus on transit systems with fixed capacitated vehicles. Only few studies have considered flexible capacity operations in transit shuttles or corridors. Our work proposes an innovative MV services in a transit network and jointly designs the dispatch headway and vehicle capacity in this network.

Second, we formulate this new problem into a new model with significant differences from the existing models in model structures. This model adds vehicle capacity decisions into the complicated transit network design problem, where interactions among different transit lines must be considered. As a result, the solution space of the problem is dramatically increased. Furthermore, the objective function of the model is nonlinear, so a mixed-integer nonlinear program is difficult to directly solve. We mathematically revise the formula to produce a computationally tractable linear model and solve both lower and upper bounds of the original nonlinear model to yield a near-optimal solution.

Third, numerical examples yield valuable managerial insights into the impacts of the proposed new transportation mode. Specifically, the MTNS is shown to be more cost effective than fixed capacity bus services in a suburban area and private car services in a highway system in China. The MTNS reduces the total system costs and critical system components (e.g., operation cost and waiting time cost) in both systems. The experiments also verify that the linearized model successfully solves near-optimal solutions to the investigated problem within an acceptable amount of time.

1 The remainder of this paper is organized as follows. Section 2 introduces the operation
 2 characteristics, notation, concept, and assumptions of the proposed MTNS. Section 3 presents the MTNS
 3 model with alternative systems. Section 4 tests the proposed model with two numerical examples in
 4 China and conducts sensitivity analyses. Finally, Section 5 provides the conclusions and recommends
 5 future research directions.

6 2. MTNS operation description

7 This section introduces the MTNS and underlying assumptions. For the convenience of the readers,
 8 the notations used throughout the paper are summarized in Table 3.

9 **Table 3 Notations**

Sets

\mathcal{J}	Set of service stations (nodes), $\mathcal{J} := \{1, \dots, I\}$
\mathcal{S}	Set of MV types, $\mathcal{S} := \{1, \dots, S\}$
\mathcal{M}	Set of a sequence of numbers, $\mathcal{M} := \{1, \dots, M\}$

Parameters

i, j, k, l	Service station index, $i, j, k, l \in \mathcal{J}$
s	MV type index, $s \in \mathcal{S}$
m	Sequence number index, $m \in \mathcal{M}$
n	Capacity of a single MV pod
ij	Link ij index for a link starting from station i ending at station j , $i, j \in \mathcal{J}$
d_{ij}	Distance of link ij , km
q_{ij}	Passenger demand from origin $i \in \mathcal{J}$ and destination $j \in \mathcal{J}$
G_{ijs}	Traffic capacity (i.e., the maximum rate of passing vehicles) on link ij specific for type- s MVs
G_{ij}	Traffic capacity on link ij , $G_{kl} = \max_{s \in \mathcal{S}} G_{kls}$
C_s	Unit-distance operation cost for type- s MV, $s \in \mathcal{S}$, \$/km
C_t	Value of time per passenger, \$/h
C_{FSBS}	Unit-distance operation cost of the fixed-capacity shuttle bus system (FSBS), \$/km
C_{PCS}	Unit-distance operation cost of the passenger car system (PCS), \$/km
v	Constant MV operating speed, km/h
β	Transfer cost per passenger, \$/h
τ_m	Waiting time of the m^{th} segment in the linearized model, $m \in \mathcal{M}$, h
F_{MTS}	System cost of the MTNS (\$)
F_{FSBS}	System cost of the FSBS (\$)
F_{PCS}	System cost of the PCS (\$)

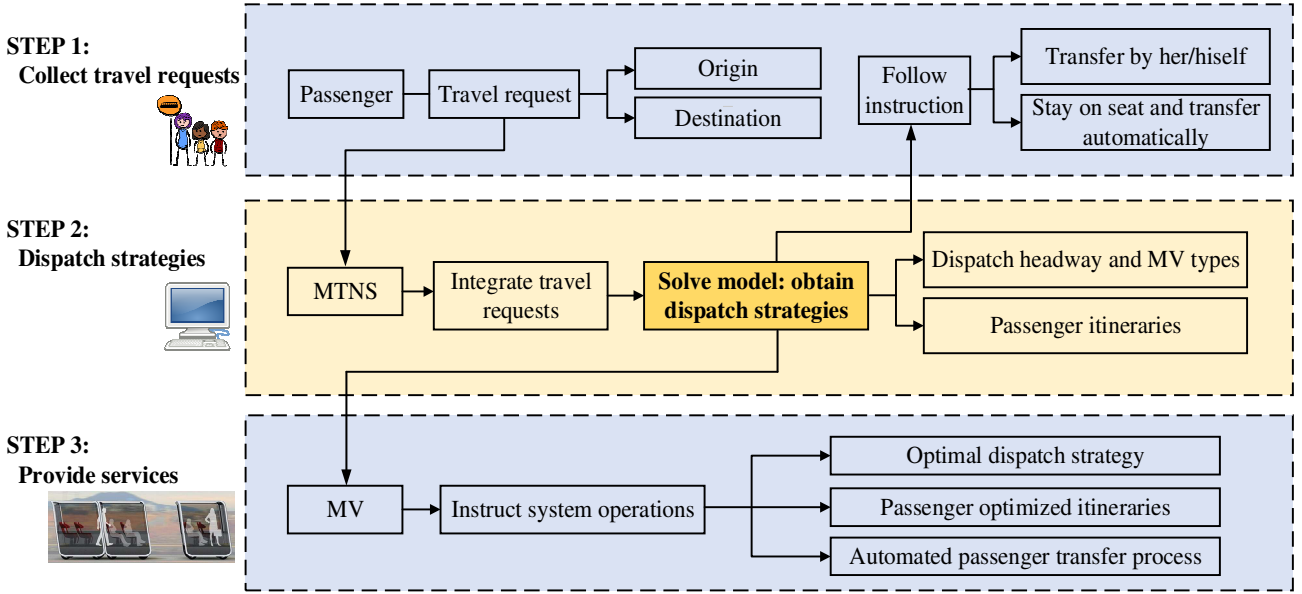
Decision variables

x_{kls}	Continuous variable; type- s MV dispatch rate from stations k to l , $x_{kls} \in \mathbb{R}^+$, $k, l \in \mathcal{J}$, $s \in \mathcal{S}$
e_{kls}	Binary variable; $e_{kls} = 1$ if MVs from station k to station l are type s ; otherwise, $e_{kls} = 0$. $k, l \in \mathcal{J}$, and $s \in \mathcal{S}$
y_{ijkl}	Continuous variable; Number of passengers traveling from stations i and j use MVs from stations k to l along their routes; $y_{ijkl} \in \mathbb{R}^+$, and $i, j, k, l \in \mathcal{J}$.
z_{klm}	Binary variable; $z_{klm} \in \{0, 1\}$, $z_{klm} = 1$ if the waiting time of MVs from stations k to l is in the range segment m ; otherwise, $z_{klm} = 0$. $k, l \in \mathcal{J}$, and $m \in \mathcal{M}$
w_{ijkl}	Continuous variable; total waiting time of passengers traveling from stations i to j that use MVs from stations k to l along their routes; $w_{ijkl} = y_{ijkl} \sum_{m \in \mathcal{M}} z_{klm} \tau_m \in \mathbb{R}^+$, and $i, j, k, l \in \mathcal{J}$.
x_{kl}^F	Continuous variable; shuttle bus dispatch rate from stations k to l ; $x_{kl}^F \in \mathbb{R}^+$, and $k, l \in \mathcal{J}$.
x_{ij}^P	Continuous variable; passenger car flow rate from stations i to j ; $x_{ij}^P \in \mathbb{R}^+$, and $i, j \in \mathcal{J}$.

Note: \mathbb{R}^+ denotes the set of nonnegative real numbers.

As Figure 2 shows, the MTNS operation is a 3-step process: collecting travel requests, optimizing

1 dispatch strategies, and providing services. First, passengers send their travel requests with their origins
 2 and destinations to a central processing system. Second, the integrated requests are fed into an
 3 optimization model (which will be presented in the next section) to solve the optimal dispatch strategy
 4 (i.e., the dispatch headway and MV types) and passenger itineraries (i.e., the MVs in which a passenger
 5 must ride to travel from the origin to the destination). Next, the optimal dispatch strategy is used to
 6 instruct system operations, and the passenger itineraries are sent to the passengers. Passengers will travel
 7 according to the optimized itineraries. Unlike the existing transit systems, the proposed MTNS adopts a
 8 fully automated passenger transfer process. Before an MV reaches a transfer station, the passengers who
 9 head to a destination station will be informed to walk to a modular pod that will eventually travel to that
 10 station if there is one. Thus, the passengers do not have to all alight the vehicle for transferring, which is
 11 expected to decrease the transfer hassle.



12
13 **Figure 2 Operation process in the MTNS**

14 The MTNS operates in a transportation network that consists of a set of stations (or nodes) \mathcal{J} , which
 15 are indexed as $i \in \mathcal{J}$ and distributed in space, and a set of links that connect pairs of stations. We denote
 16 a link starting from station $i \in \mathcal{J}$ and ending at station $j \in \mathcal{J}$ as (i, j) and its length as d_{ij} . Let q_{ij} denote
 17 the passenger demand from origin $i \in \mathcal{J}$ to destination $j \in \mathcal{J}$, and we assume that this demand remains
 18 constant throughout the investigated period in this problem. We denote the set of MV types that can be
 19 dispatched to serve the passengers as $\mathcal{S} := \{1, \dots, S\}$, which are indexed as $s \in \mathcal{S}$. A type- s MV has s
 20 modular pods and a capacity of sn , where n is the capacity of a single pod. During the operation, MVs
 21 flexibly adjust the vehicle capacity via docking/undocking to satisfy the passenger demand. This process
 22 can be manually or, in the future, automatically controlled.

23 To better understand the potential benefits of the MTNS, let us consider a simple illustrative
 24 example. Figure 3 shows an example with five service stations ($\mathcal{J} = \{1, \dots, 5\}$) and six types of MVs
 25 ($\mathcal{S} = \{1, \dots, 6\}$). In this figure, on each link between two stations, the arrows of different colors represent
 26 different MV types, and the line weights represent the MV dispatch frequencies. The OD pairs and
 27 sampled demands associated with station 4 are listed in Table 4. The optimal operation strategy of
 28 station 4 is also presented in Table 4. Some passengers take direct MVs without transfers (e.g., $1 \rightarrow$
 29 $4, 2 \rightarrow 4, 5 \rightarrow 4, 4 \rightarrow 1$, and $4 \rightarrow 5$), and other passengers make multiple transfers to complete the trip
 30 (e.g., $3 \rightarrow 5 \rightarrow 4, 4 \rightarrow 5 \rightarrow 1, 4 \rightarrow 5 \rightarrow 2, 4 \rightarrow 5 \rightarrow 3$). Moreover, passengers with identical origins and

destinations may take multiple routes. For example, for OD 4 → 1, 7.79% of passengers take route 4 → 5 → 1 with an average waiting time of 0.154 h for the first segment and 0.22 h for the second segment, and 92.21% of passengers instead take route 4 → 1 with an average waiting time of 0.154 h.

Table 4 Optimal operation strategies for station 4

Station		4	OD pairs	Demands (q_{ij})	Optimal operation strategies	Optimal vehicle type (s)	Average waiting time ($\frac{1}{2 * x_{kls}}$)
Number of pots s=1 s=2 s=3 s=4 s=5 s=6	1	5	1 → 4	22	1 → 4	2	0.198
			2 → 4	15	2 → 4	1	0.2
			3 → 4	10	3 → 5 → 4	4; 4	0.42; 0.22
			5 → 4	23	5 → 4	4	0.22
			4 → 1	21	4 → 1	1	0.154
					4 → 5 → 1	6; 4	0.154; 0.22
2	3		4 → 2	45	4 → 5 → 2	6; 4	0.154; 0.218
			4 → 3	11	4 → 5 → 3	6; 5	0.154; 0.211
			4 → 5	22	4 → 5	6	0.22

Figure 3 Illustration of optimal MTNS operations

Finally, to facilitate the model formulation, we introduce the following assumptions in the investigated problem.

Assumption 1. The demands are stationary over the investigated time period. The assumption of static traffic flow patterns is commonly adopted in transportation network modeling. Moreover, the passenger arrival follows the random distribution. Thus, the average passenger waiting time is half of the headway, which has been widely used in the waiting time cost estimation (Ansari Esfeh et al., 2020).

Assumption 2. All passengers waiting at a station follow the transfer policy specified in the MTNS. Each link ij has a traffic capacity (i.e., the maximum rate of passing vehicles) G_{ijs} specific to each type- s MV. Since different types of MVs have different lengths, MVs may have type-specific traffic capacities on the same link.

Assumption 3. Only one type of MVs can operate on a link. This assumption is made to ensure the computational tractability of the model. This assumption is reasonable, since a stationary traffic flow on a link is likely associated with one optimal MV configuration.

Assumption 4. Each station has sufficient space to store the reserved pods to off-set local demand perturbations at the station. This assumption ensures that each station always dispatch MVs on schedule according to the optimal dispatch frequency, even with local demand perturbations, and ensures that the pods are sufficient. Thus, we do not pose a fleet size constraint on the system operation and can dispatch as many vehicles as necessary. We also do not have to consider the vehicle dwell time and the cost for vehicle purchase and maintenance. The fleet planning problem is relevant, but it belongs to the planning stage and can be separated from the operational problem. The optimal fleet size can be determined after the operational plan has been solved.

Assumption 5. Congestion is not considered, since only a small portion of the demand takes the proposed service, which will hardly impact the road network congestion patterns. Thus, the system design will not affect the travel time of each link.

3. Methodology

This section provides model formulations for the investigated and related benchmark systems.

1 3.1 Model formulation for the MTNS system

2 3.1.1 Original model formulation

3 The investigated problem involves optimizing the vehicle dispatch strategy (specified by x_{kls} and
4 e_{kls}) and passenger itineraries (specified by y_{ijkl}) to minimize the total system cost. We first introduce
5 the following decision variables in the MTNS:

- 6 • x_{kls} : Continuous variable x_{kls} denotes the dispatch rate of type- s MVs from stations k to l . We assume
7 that the traffic demand on any link is much higher than the capacity of an MV; thus, without
8 much loss of generality, x_{kls} is set as a continuous decision variable.
- 9 • y_{ijkl} : Continuous variable y_{ijkl} denotes the rate of passengers who travel from stations i and j using
10 MVs from stations k to l along their routes. This flexible notation allows a passenger to transfer
11 across multiple MV links to complete a trip if it is favorable for the passenger.
- 12 • e_{kls} : Binary variable e_{kls} denotes whether the MVs from stations k to l are type s . If yes, $e_{kls} = 1$;
13 otherwise, $e_{kls} = 0$.

14 *Objective function*

15 The objective function formulated in Equation (1) aims to minimize the overall system cost, which
16 consists of two components: operation cost and passenger trip time cost. The passenger trip time cost
17 can be calculated by the passenger waiting cost, riding time cost (in-vehicle travel cost), and transfer
18 penalties. Let C_s denote the operation cost of each type- s MV per unit distance; the operation cost
19 includes the MV depreciation, maintenance, infrastructure investment, electricity, and fuel costs. With
20 the unit-distance operation cost C_s , the unit-time operation cost for all type- s MVs in the system is
21 simply a product of C_s and the total travel distance per unit time, $\sum_{k \in \mathcal{J}, l \in \mathcal{J}} x_{kls} d_{kl}$. This operation yields
22 the system operation cost as $\sum_{k \in \mathcal{J}, l \in \mathcal{J}, s \in \mathcal{S}} C_s x_{kls} d_{kl}$, as the first term of Equation (1) specifies. Let C_t
23 denote the value of time per passenger. With this, the passenger trip time cost, including the passenger
24 waiting time and riding time, is formulated as the second term of Equation (2). Specifically, the average
25 waiting time of a passenger riding an MV on link kl is $\frac{1}{2 \sum_{s \in \mathcal{S}} x_{kls}}$, where $\sum_{s \in \mathcal{S}} x_{kls}$ is the MV dispatch
26 frequency on link kl (Assumption 1). For mathematical convenience, we define $\frac{1}{2 \sum_{s \in \mathcal{S}} x_{kls}}$ as a large
27 value when $\sum_{s \in \mathcal{S}} x_{kls}$ approaches 0. Next, with a constant MV operating speed v , the riding time for a
28 passenger riding an MV on link kl is $\frac{d_{kl}}{v}$. Furthermore, let β denote the extra cost for a passenger to
29 make one additional transfer to capture hassles during the transfer process. The extra cost due to the
30 splitting and reassembling operations of MVs can be included in parameter β . Thus, the total transfer
31 cost for the passenger throughout the trip is the product of β and the total number of transfers. During a
32 trip, a passenger makes exactly one additional transfer at each leg except the first leg, so the total
33 number of transfers throughout the passenger's trip is $\sum_{i \in \mathcal{J}, j \in \mathcal{J}, k \neq i \in \mathcal{J}, l \in \mathcal{J}} y_{ijkl}$. This approach yields the
34 transfer penalty as the third term in Equation (1). Although the en-route transfer operations of MV may
35 reduce the transfer hassle, passengers may still have to wait before the vehicle leaves the transfer station
36 because of the asynchrony. Thus, objective function (1) incorporates the costs related to the transfer
37 process, which include the transfer cost caused by the transfer time (which is incorporated in the waiting
38 time cost) and transfer inconvenience cost (which is formulated as the transfer penalty component in the
39 objective function). These components also quantify the tradeoff between serving passengers with more
40 direct services (i.e., more vehicles) and more transfers (i.e., fewer vehicles) in the system.

$$\begin{aligned}
\min_{x_{kls}, y_{ijkl}, e_{kls}} F_{MTS} := & \sum_{k \in \mathcal{J}, l \in \mathcal{J}, s \in \mathcal{S}} C_s x_{kls} d_{kl} + \sum_{i \in \mathcal{J}, j \in \mathcal{J}, k \in \mathcal{J}, l \in \mathcal{J}} C_t y_{ijkl} \left(\frac{1}{2 \sum_{s \in \mathcal{S}} x_{kls}} + \frac{d_{kl}}{v} \right) \\
& + \sum_{i \in \mathcal{J}, j \in \mathcal{J}, k \neq i \in \mathcal{J}, l \in \mathcal{J}} \beta y_{ijkl}
\end{aligned} \tag{1}$$

1 Constraints

2 We consider four groups of constraints in the MTNS: vehicle capacity Constraint (2), pod
3 conservation Constraint (3), passenger flow conservation Constraints (4)-(6), and unique MV type
4 Constraints (7)-(8).

$$\sum_{i \in \mathcal{J}, j \in \mathcal{J}} y_{ijkl} \leq \sum_{s \in \mathcal{S}} x_{kls} s n \quad \forall k, l \in \mathcal{J} \quad \text{Vehicle capacity constraint} \tag{2}$$

$$\sum_{k \in \mathcal{J} \setminus \{l\}, s \in \mathcal{S}} x_{kls} s = \sum_{k \in \mathcal{J} \setminus \{l\}, s \in \mathcal{S}} x_{lks} s \quad \forall l \in \mathcal{J} \quad \text{Pod conservation constraint} \tag{3}$$

$$\sum_{l \in \mathcal{J} \setminus \{i\}} y_{ijil} = q_{ij} \quad \forall i, j \in \mathcal{J} \quad \text{Passenger flow conservation constraint} \tag{4}$$

$$\sum_{k \in \mathcal{J} \setminus \{j\}} y_{ijkj} = q_{ij} \quad \forall i, j \in \mathcal{J} \quad \text{Passenger flow conservation constraint} \tag{5}$$

$$\sum_{k \in \mathcal{J}} y_{ijkl} = \sum_{k \in \mathcal{J}} y_{ijlk} \quad \forall l \in \mathcal{J} \setminus \{i, j\}, i, j \in \mathcal{J} \quad \text{Passenger flow conservation constraint} \tag{6}$$

$$\sum_{s \in \mathcal{S}} e_{kls} = 1 \quad \forall k, l \in \mathcal{J} \quad \text{Unique MV type constraint} \tag{7}$$

$$x_{kls} \leq e_{kls} G_{kls} \quad \forall k, l \in \mathcal{J}, s \in \mathcal{S} \quad \text{Unique MV type constraint} \tag{8}$$

$$x_{kls} \in \mathbb{R}^+ \cup \{0\} \quad \forall k, l \in \mathcal{J}, \text{ and } s \in \mathcal{S} \quad \text{Variable domain} \tag{9}$$

$$y_{ijkl} \in \mathbb{R}^+ \cup \{0\} \quad \forall i, j, k, l \in \mathcal{J} \quad \text{Variable domain} \tag{10}$$

$$e_{kls} \in \mathbb{B} \quad \forall k, l \in \mathcal{J}, \text{ and } s \in \mathcal{S} \quad \text{Variable domain} \tag{11}$$

5 Constraint (2) is the vehicle capacity constraint, which mandates that for each link kl , the total MV
6 capacity (shown on the right-hand side, abbr. RHS) is sufficient to serve all passengers using this link
7 (shown on the left-hand side, abbr. LHS). Constraint (3) involves the conservation of the MV pods
8 circulating in the system; i.e., the total number of MV pods that arrive at each station l (LHS) is identical
9 to the total number of MV pods that depart from station l per unit time (RHS). This pod conservation
10 constraint ensures that the vehicles are balanced; i.e., the total number of modular pods in the system
11 remains constant throughout the operation. However, the vehicle balance does not necessarily equate to
12 passenger flow balance, so the model allows imbalanced passenger flows at a station. Constraints (4),
13 (5), and (6) are related to the conservation of passenger flows. Constraint (4) requires all passengers
14 traveling between origin i and destination j must leave origin i . Likewise, Constraint (5) imposes that all
15 passengers traveling between origin i and destination j must arrive at destination j . Constraint (6)
16 indicates that for each station l , the number of passengers arriving at station l (LHS) must equal that
17 leaving station l (RHS). Constraint (7) limits only one type of MV to serve link kl . Constraint (8)
18 specifies that the MV flow on each link should not exceed the traffic capacity. Constraints (9), (10) and
19 (11) are the variable domains.

1 3.1.2 Linearization approximation

2 In objective function (1), the waiting time cost term $\sum_{i \in \mathcal{J}, j \in \mathcal{J}, k \in \mathcal{J}, l \in \mathcal{J}} C_t y_{ijkl} \frac{1}{2 \sum_{s \in \mathcal{S}} x_{kls}}$ is biconvex,
 3 since both $\sum_{i \in \mathcal{J}, j \in \mathcal{J}, k \in \mathcal{J}, l \in \mathcal{J}} y_{ijkl}$ and $\sum_{k \in \mathcal{J}, l \in \mathcal{J}} \frac{1}{2 \sum_{s \in \mathcal{S}} x_{kls}}$ are convex functions of the corresponding decision
 4 variables. It is commonly known that mathematical programming problems with biconvex terms are
 5 difficult to directly solve (Gorski et al., 2007; Liberti and Pantelides, 2006). To facilitate the solution
 6 approach, this section reformulates the waiting time cost component as a linear term via two steps.

7 *Step 1: Bilinear model reformulation*

8 We first reformulate the waiting time cost term as a bilinear term by dividing the feasible region of
 9 the waiting time into M segments. We construct an arithmetic sequence $\tau_1, \tau_2, \dots, \tau_m, \dots, \tau_M$ that satisfies
 10 $\tau_1 \leq \frac{1}{2 \sum_{s \in \mathcal{S}} x_{kls}} < \tau_M$. This sequence can be dynamically changed to reach a lower approximation error
 11 (i.e., the difference between approximated and original objective values). Then, we introduce binary
 12 variables $z_{klm} := \{0,1\}, k, l \in \mathcal{J}, m \in \mathcal{M}$ to denote whether the waiting time of MVs on link kl is in the
 13 range of the m^{th} segment. In other words, we set $z_{klm} = 1$ if $\exists m \in \mathcal{M} \setminus \{M\}, s.t. \tau_m \leq \frac{1}{2 \sum_{s \in \mathcal{S}} x_{kls}} <$
 14 τ_{m+1} ; otherwise, $z_{klm} = 0$. Then, $\frac{1}{2 \sum_{s \in \mathcal{S}} x_{kls}}$ is linearized to $\sum_{m \in \mathcal{M}} z_{klm} \tau_m$, and
 15 $\sum_{i \in \mathcal{J}, j \in \mathcal{J}, k \in \mathcal{J}, l \in \mathcal{J}} C_t y_{ijkl} \frac{1}{2 \sum_{s \in \mathcal{S}} x_{kls}}$ in the original objective function is reformulated to a bilinear component
 16 $\sum_{i \in \mathcal{J}, j \in \mathcal{J}, k \in \mathcal{J}, l \in \mathcal{J}} C_t y_{ijkl} \sum_{m \in \mathcal{M}} z_{klm} \tau_m$ subject to linearization Constraints (12)-(15). Constraint (12)
 17 postulates that the waiting time can occupy one and only one segment of the time intervals with $z_{klm} =$
 18 1, e.g., $[\tau_m, \tau_{m+1})$. Let G_{kl} denotes the traffic capacity on link ij ($G_{kl} = \max_{s \in \mathcal{S}} G_{kls}$). As Assumption 2
 19 shows, each link kl has a traffic capacity G_{kls} (i.e., the maximum rate of passing vehicles) specific to
 20 type s . Constraints (13) and (14) specify that the value of $2 \sum_{s \in \mathcal{S}} x_{kls}$ falls above $1/\tau_{m+1}$ and below
 21 (inclusive) $1/\tau_m$ to be consistent with $\tau_m \leq \frac{1}{2 \sum_{s \in \mathcal{S}} x_{kls}} < \tau_{m+1}$. Constraints (13) and (14) are activated
 22 only when $z_{klm} = 1$ to ensure that z_{klm} indicates the correct time interval segment. Constraint (15)
 23 specifies z_{klm} as a binary variable.

$$\sum_{m \in \mathcal{M}} z_{klm} = 1 \quad \forall k, l \in \mathcal{J} \quad (12)$$

$$2 \sum_{s \in \mathcal{S}} x_{kls} > 2G_{kl}(z_{klm} - 1) + \frac{1}{\tau_{m+1}} \quad \forall k, l \in \mathcal{J}, m \in \mathcal{M} \quad (13)$$

$$2 \sum_{s \in \mathcal{S}} x_{kls} \leq \frac{1}{\tau_m} + 2G_{kl}(1 - z_{klm}) \quad \forall k, l \in \mathcal{J}, m \in \mathcal{M} \quad (14)$$

$$z_{klm} \in \{0,1\} \quad \forall k, l \in \mathcal{J}, m \in \mathcal{M} \quad (15)$$

24 *Step 2: Linear model reformulation*

25 Since the waiting time component in *step 1*, $\sum_{i \in \mathcal{J}, j \in \mathcal{J}, k \in \mathcal{J}, l \in \mathcal{J}} y_{ijkl} \sum_{m \in \mathcal{M}} z_{klm} \tau_m$, is a bilinear term
 26 that remains challenging to solve, we further linearize this term. Here, we introduce continuous variables
 27 $w_{ijkl} \in \mathbb{R}^+, i, j, k, l \in \mathcal{J}$. Then, we revise the bilinear term to $\sum_{i \in \mathcal{J}, j \in \mathcal{J}, k \in \mathcal{J}, l \in \mathcal{J}} C_t w_{ijkl}$ as a linear term with
 28 the following constraints. Constraints (16) and (17) ensure that the value of w_{ijkl} is identical to
 29 $\sum_{m \in \mathcal{M}} z_{klm} y_{ijkl} \tau_m$. The reason is that when $z_{klm} = 0$, Constraints (16) and (17) always hold for all
 30 feasible values of w_{ijkl} allowed by the demand and consequently are not activated; only when $z_{klm} = 1$,

1 Constraint (16) yields $y_{ijkl}\tau_m \leq w_{ijkl}$, and Constraint (17) yields $w_{ijkl} \leq y_{ijkl}\tau_m$; thus, $w_{ijkl} =$
 2 $y_{ijkl}\tau_m$. Constraint (18) specifies each w_{ijkl} as a nonnegative continuous variable.

$$y_{ijkl}\tau_m - q_{ij}\tau_m(1 - z_{klm}) \leq w_{ijkl} \quad \forall i, j, k, l \in \mathcal{J}, m \in \mathcal{M} \quad (16)$$

$$w_{ijkl} \leq y_{ijkl}\tau_m + q_{ij}\tau_m(1 - z_{klm}) \quad \forall i, j, k, l \in \mathcal{J}, m \in \mathcal{M} \quad (17)$$

$$w_{ijkl} \in \mathbb{R}^+ \cup \{0\} \quad \forall i, j, k, l \in \mathcal{J} \quad (18)$$

3 With these linearization steps, the investigated MTNS problem is reformulated as the following
 4 MILP model with objective (19), subject to vehicle capacity Constraint (2), pod conservation Constraint
 5 (3), passenger flow conservation Constraints (4)-(6), unique MV type Constraints (7)-(8), linearization
 6 Constraints (12)-(14) and (16)-(17), and variable domain Constraints (9)-(11), (15), and (18):

$$\begin{aligned} \min_{x_{kls}, y_{ijkl}, e_{kls}, z_{klm}, w_{ijkl}} F_{MTS} := & \sum_{k \in \mathcal{J}, l \in \mathcal{J}, s \in \mathcal{S}} C_s x_{kls} d_{kl} \\ & + C_t \left(\sum_{i \in \mathcal{J}, j \in \mathcal{J}, k \in \mathcal{J}, l \in \mathcal{J}} w_{ijkl} + \sum_{i \in \mathcal{J}, j \in \mathcal{J}, k \in \mathcal{J}, l \in \mathcal{J}} y_{ijkl} \frac{d_{kl}}{v} \right) \\ & + \sum_{i \in \mathcal{J}, j \in \mathcal{J}, k \neq i \in \mathcal{J}, l \in \mathcal{J}} \beta y_{ijkl} \end{aligned} \quad (19)$$

s. t. constraints (2) – (18)

7 The above process successfully revises the original nonlinear model (NLM) to a linear model (LM),
 8 reduces the solution complexity and enables the model to be solved with a mixed linear integer
 9 programming solver. However, an approximation error ensues from the revision of the waiting time cost
 10 term in the LM. The following theoretical properties of the relationship between NLM and LM solutions
 11 are shown to quantify the approximation error.

12 **Theorem 1.** The optimal objective value of the LM is a lower bound to that of the NLM.

13 **Proof.** For the NLM, we denote the optimal solution to variables $\{x_{kls}, y_{ijkl}, e_{kls}\}$ as
 14 $\{x_{kls}^*, y_{ijkl}^*, e_{kls}^*\}$ and the associated optimal objective value as F_{NLM}^* , which is the value of Equation (1)
 15 after substituting $\{x_{kls}^*, y_{ijkl}^*, e_{kls}^*\}$.

16 By substituting the dispatch solution $\{x_{kls}^*, y_{ijkl}^*, e_{kls}^*\}$ into Constraints (12) and (18), we can solve
 17 the corresponding $\{z_{klm}, w_{ijkl}\}$ values, which are denoted as $\{z_{klm}^*, w_{ijkl}^*\}$. Obviously,
 18 $\{x_{kls}^*, y_{ijkl}^*, e_{kls}^*, z_{klm}^*, w_{ijkl}^*\}$ is a feasible solution to the LM, and we denote the corresponding objective
 19 value, i.e., the value of Equation (19) after substituting $\{x_{kls}^*, y_{ijkl}^*, e_{kls}^*, z_{klm}^*, w_{ijkl}^*\}$, as F_{LM} .

20 Then, we obtain

$$F_{\text{NLM}}^* - F_{\text{LM}} = C_t * \sum_{i \in \mathcal{J}, j \in \mathcal{J}, k \in \mathcal{J}, l \in \mathcal{J}} y_{ijkl} \frac{1}{2 \sum_{s \in \mathcal{S}} x_{kls}} - \sum_{i \in \mathcal{J}, j \in \mathcal{J}, k \in \mathcal{J}, l \in \mathcal{J}} w_{ijkl}.$$

22 Since Constraints (16) and (18) ensure that the value of w_{ijkl} is identical to $\sum_{m \in \mathcal{M}} z_{klm} y_{ijkl} \tau_m$, $F_{\text{NLM}}^* -$
 23 F_{L} can be reformulated as follows:

$$F_{\text{NLM}}^* - F_{\text{LM}} = C_t * \sum_{i \in \mathcal{J}, j \in \mathcal{J}, k \in \mathcal{J}, l \in \mathcal{J}} y_{ijkl} \left(\frac{1}{2 \sum_{s \in \mathcal{S}} x_{kls}} - \sum_{m \in \mathcal{M}} z_{klm} \tau_m \right).$$

1 Constraints (12)-(15) ensure that the value of $\frac{1}{2 \sum_{s \in S} x_{kls}}$ falls between τ_m and τ_{m+1} for the m value with
 2 $z_{klm} = 1$. It obviously indicates that $\frac{1}{2 \sum_{s \in S} x_{kls}} \geq \sum_{m \in \mathcal{M}} z_{klm} \tau_m$ and consequentially $F_{\text{NLM}}^* \geq F_{\text{LM}}$.

3 By definition, the objective value F_{LM} corresponding to any feasible solution to the LM is not less
 4 than its optimal objective value, denoted as F_{LM}^* , which yields $F_{\text{NLM}}^* \geq F_{\text{LM}}^*$. This completes the proof.

5 **Theorem 2.** Let $\{x'_{kls}, y'_{ijkl}, e'_{kls}, z'_{klm}, w'_{ijkl}\}$ denote the optimal solution to the LM. Then,
 6 $\{x'_{kls}, y'_{ijkl}, e'_{kls}\}$ is a feasible solution to the NLM, and the corresponding objective value, i.e., the value
 7 of Equation (1) after substituting $\{x'_{kls}, y'_{ijkl}, e'_{kls}\}$, which is denoted by F'_{NLM} , constitutes an upper
 8 bound to the optimal objective value of the NLM, F_{NLM}^* .

9 **Proof.** The linearization process successfully revises the original NLM to an LM by reformulating
 10 the nonlinear component to a linear term and adding a series of new linear Constraints (12)-(18). Since
 11 the LM and NLM share the same Constraints (2)-(11), the solution $\{x'_{kls}, y'_{ijkl}, e'_{kls}\}$, which is optimal
 12 and feasible in the LM, is also feasible in the NLM. Then, F'_{NLM} is a feasible objective value of the
 13 NLM, so $F'_{\text{NLM}} \geq F_{\text{NLM}}^*$. Here, we complete the proof.

14 With the above theoretical properties, by solving the optimal solution to the LM, we obtain a set of
 15 near-optimal solutions to the NLM (i.e., $\{x'_{kls}, y'_{ijkl}, e'_{kls}\}$ with objective value F'_{NLM}) and a lower bound
 16 of the optimal objective value (i.e., F_{LM}^*). The optimality gap of the near-optimal solution can be
 17 evaluated as $(F'_{\text{NLM}} - F_{\text{LM}}^*) / F_{\text{LM}}^*$. The approximation error between NLM and LM is determined by the
 18 sizes of the intervals $\{[\tau_m, \tau_{m+1}]\}$ that contain the corresponding $\left\{\frac{1}{2 \sum_{s \in S} x_{kls}}\right\}$ values. Thus, to reduce the
 19 approximation error, we may redistribute the $\{\tau_m\}$ values according to the obtained $\{x_{kls}\}$ solutions as
 20 follows.

- 21 a) Evenly divide $[0, \tau_M]$ into M intervals to solve the LM. This step produces the LM solution and
 22 system cost. Then, substitute the LM solution into Equation (1) to calculate the corresponding
 23 NLM objective value.
- 24 b) Gather the values of $\{x_{kls}\}$ in the LM solution into k clusters and redistribute the $\{\tau_m\}$ values
 25 with a higher density around each cluster.
- 26 c) Solve the LM again with the new $\{\tau_m\}$ values.

27 This process can be repeated until the approximation error is acceptable. While these three steps update
 28 the values of $\{\tau_m\}$, they do not affect the validity of Theorems 1 and 2, since the theorems take $\{\tau_m\}$ as a
 29 set of input parameters that can be given any values.

30 3.2 Alternative systems

31 To compare with the proposed MTNS, this section describes two benchmark systems: the fixed-
 32 capacity shuttle bus system (FSBS) and the passenger car system (PCS). We adapt the above MTNS
 33 model to specify the FSBS and PCS as flows based on the related characteristics. There are many
 34 different possible benchmark systems to compare with the proposed MTNS. However, it is not possible
 35 to enumerate each system in one study, since solving the optimal design for each system is very
 36 challenging. Here, we simply select two existing benchmark systems to reveal the benefits of the flexible
 37 capacity operations in the MTNS. More studies are required to fully understand its advantages over
 38 other systems.

39 In the FSBS, each vehicle has a fixed capacity of n^F and provides direct point-to-point
 40 transportation without intermediate stops. Let C_{FSBS} denote the FSBS operation cost per distance. The
 41 FSBS model can be obtained by replacing x_{kls} with x_{kl}^F (denoting the shuttle bus dispatch rate on link

1 kl in objective function (20), vehicle capacity Constraint (21), pod conservation Constraint (22), and
 2 other Constraints (3)-(6), (9), and (12)-(18) as follows:

$$\begin{aligned} \min_{x_{kl}^F, y_{ijkl}, e_{kls}} F_{FSBS} := & \sum_{k \in \mathcal{J}, l \in \mathcal{J}} C_{FSBS} x_{kl}^F d_{kl} + \sum_{i \in \mathcal{J}, j \in \mathcal{J}, k \in \mathcal{J}, l \in \mathcal{J}} C_t y_{ijkl} \left(\frac{1}{2x_{kl}^F} + \frac{d_{kl}}{v} \right) \\ & + \sum_{i \in \mathcal{J}, j \in \mathcal{J}, k \neq i \in \mathcal{J}, l \in \mathcal{J}} \beta y_{ijkl} \end{aligned} \quad (20)$$

s. t. constraints (3) – (6), (9), (12) – (18)

$$\sum_{i \in \mathcal{J}, j \in \mathcal{J}} y_{ijkl} \leq x_{kl}^F n^F \quad \forall k \in \mathcal{J}, l \in \mathcal{J} \quad (21)$$

$$\sum_{k \in \mathcal{J} \setminus \{l\}} x_{kl}^F = \sum_{k \in \mathcal{J} \setminus \{l\}} x_{lk}^F \quad \forall l \in \mathcal{J} \quad (22)$$

$$x_{kl}^F \in \mathbb{R}^+ \cup \{0\} \quad \forall k \in \mathcal{J}, l \in \mathcal{J} \quad (23)$$

3 In the PCS, where private passenger cars and taxis dominate, each vehicle has a small average
 4 occupancy of n^P . Let C_{PCS} denote the PCS operation cost per distance. The PCS considers an idealized
 5 situation where taxis and private vehicles directly transport passengers from their origins to their
 6 destinations without transfers, which eliminates the need for waiting at the origins or transfer points.
 7 Thus, the system cost includes only the operation cost and passenger riding time cost from the origin to
 8 the destination. With this approach, the PCS model can be obtained by replacing x_{kls} with x_{ij}^P (denoting
 9 the passenger car flow rate on link ij) in objective (24), pod conservation Constraint (25), passenger
 10 flow conservation Constraint (27), and variable domain Constraints (28)-(29) as follows:

$$\min_{x_{ij}^P, y_{ijkl}, e_{kls}} F_{PCS} := \sum_{i \in \mathcal{J}, j \in \mathcal{J}} C_{PCS} x_{ij}^P d_{kl} + \sum_{i \in \mathcal{J}, j \in \mathcal{J}} C_t y_{ijij} \frac{d_{ij}}{v} \quad (24)$$

s. t.

$$y_{ijij} \leq x_{ij}^P n^P \quad \forall i \in \mathcal{J}, j \in \mathcal{J} \quad (25)$$

$$\sum_{i \in \mathcal{J} \setminus \{j\}} x_{ij}^P = \sum_{j \in \mathcal{J} \setminus \{i\}} x_{ji}^P \quad \forall j \in \mathcal{J} \quad (26)$$

$$y_{ijij} = q_{ij} \quad \forall i \in \mathcal{J}, j \in \mathcal{J} \quad (27)$$

$$x_{ij}^P \in \mathbb{R}^+ \cup \{0\} \quad \forall i \in \mathcal{J}, j \in \mathcal{J} \quad (28)$$

$$y_{ijij} \in \mathbb{R}^+ \cup \{0\} \quad \forall i \in \mathcal{J}, j \in \mathcal{J} \quad (29)$$

11 4. Numerical example

12 To illustrate the application of the proposed MTNS model, this section explores two numerical
 13 examples with different network sizes. All experiments were performed on an Intel® Core™ i7-8550U
 14 1.99 GHz CPU with 24 GB of RAM. The code was implemented in MATLAB 2019a and called a
 15 commercial MILP solver Gurobi (Cochran et al., 2011; Fuentes et al., 2019; Zhang et al., 2019) to solve
 16 the linearized model. The default parameter values are set as follows.

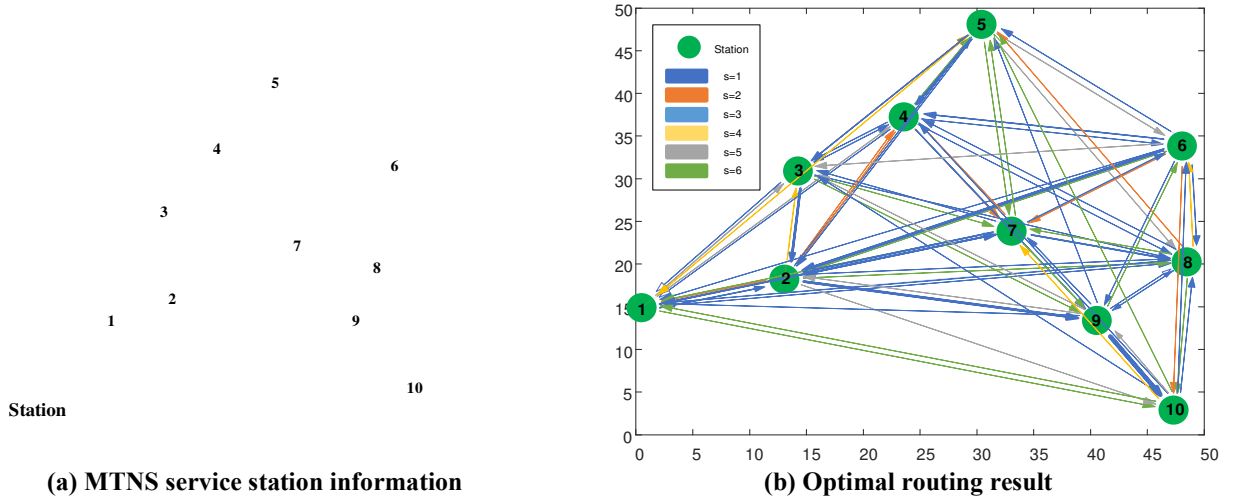
17 **Table 5 Default parameter settings**

Parameter	Value	Data source
\mathcal{S}	[1, 2, 3, 4, 5, 6]	NEXT website (https://www.next-future-mobility.com)
n	6 passengers	NEXT website (https://www.next-future-mobility.com)

n^F	36 passengers	Guangzhou No. 3 Bus Company (http://www.bus3.cn/sitecn/msg.aspx)
n^P	1.5 passengers	Freeway operation report of Guangdong Province, China (http://data.eastmoney.com/notices/detail/)
C_s	[0.143, 0.257, 0.347, 0.417, 0.471, 0.514] \$/km	Operation cost is not a linear function of the number of dispatched pods; NEXT website (https://www.next-future-mobility.com)
C_{FFBS}	0.514 \$/km	Guangzhou No. 3 Bus Company
C_{PTS}	0.143 \$/km	Guangzhou Taxi Company
C_t	2.86 \$/h in Guangzhou	Guangzhou Municipal Human Resources and Social Security Bureau reports in 2019 (http://gzrsj.hrssgz.gov.cn/english/)
β	0.142 \$/passenger	Passenger transfer cost are determined by referring to the average income per capita from Guangzhou Municipal Human Resources and Social Security Bureau reports in 2019.
v	31.85 km/h	Operating speed of MVs on city roads (case 1) (http://www.gzjt.gov.cn/gzjt/)
	60.32 km/h	Operating speed of MVs on the freeway (case 2) (http://www.0512s.com/lukuang/)

1 4.1 Ten-station example

2 Example 1 is a public transit system in Guangzhou Higher Education Mega Center, China. As shown
3 in Figure 4 (a), we selected 10 critical bus stops and collected the real-world travel demand data for each
4 stop to investigate this example. The bus stops in this system are sparse and scattered, and it is
5 uneconomic to form a transit corridor because of the long deviation cost. The travel demand data and
6 road distance data were obtained from the Communications Commission of Guangzhou Municipality. In
7 addition to the default parameter values specified in Table 1, we set $M = 20$ and $\tau = [0.02: 0.01: 0.1,$
8 $0.2: 0.1: 1, 500, 1000]$ after extensive experiments. The optimal solution (exact solution) of the proposed
9 model is obtained within 0.12 h. The optimal MTNS service strategy is shown in Figure 4(b). Different
10 colors represent different MV types, and the thickness of each arrow illustrates the frequency of the
11 modular vehicle fleet on the corresponding link.



12 (a) MTNS service station information
13 Figure 4 Numerical example from Guangzhou, China

14 Cost comparisons

15 We compared the MTNS solutions with those from the FSBS and PCS alternatives. The number of
16 modular pods in the FSBS vehicles is set to the optimal value of $S = 6$ (see Figure 5(e) for why this is
17 optimal). In this experiment, we used the system cost (which includes the operation cost, waiting time
18 cost, riding time cost, and transfer cost) as the criterion to evaluate the performance of different systems.

1 The results are shown in Table 6, where the percentage of cost reduction is calculated as $\frac{F_{FSBS}-F_{MTS}}{F_{MTS}} * 100\%$ and $\frac{F_{PTS}-F_{MTS}}{F_{MTS}} * 100\%$.

3 The total system cost in the MTNS is less than those in the FSBS and PCS. The MTNS reduces the
 4 system cost by 7.10% and 28.96% compared to the FSBS and PCS, respectively. The cost savings are
 5 more pronounced when we remove the fixed free-flow travel time independent of the optimal decisions.
 6 In other words, the revised system cost reduction becomes 31.39% and 128.03% compared to the FSB
 7 and PCS. The comparison between MTNS and FSBS shows that a flexible capacity transit system
 8 performs better than a fixed system. The benefits of the MNTS may not be as evident when we compare
 9 it with a transit network system where different lines operate with vehicles of different sizes (e.g., vans,
 10 minibuses). This comparison is not offered here, since it requires us to solve another optimal system
 11 design problem with the capacities of different lines as decision variables. This problem is non-trivial
 12 and out of the scope of this paper. Thus, the results here only offer an upper bound to the benefits of the
 13 proposed MNTS with existing transit operations.

14 Regarding the system cost components, the reduction in operation cost (33.63%) is maximal when we
 15 compare the MTNS with the FSBS because the flexible vehicle capacity in the MTNS promotes frequent
 16 dispatching of small vehicles. In contrast, the FSBS can only dispatch vehicles with a stationary capacity
 17 and lead to a frequent rate. The improvements in riding costs are relatively minor, likely because the
 18 waiting time at the origin and transfer points is much less than the in-vehicle travel time overall, which
 19 is nearly 77% in this example. Although the in-vehicle travel time cost does not dramatically change, the
 20 bulk of the riding time cost is dominated by the travel distance and independent of the transportation
 21 system. If we remove the fixed free-flow travel time, we see a much more significant improvement in
 22 the variable riding time cost affected by the transportation system settings. For reference, Table 6
 23 provides the revised riding time cost, which is reduced by 1983.78%. Additionally, compared to the
 24 MTNS, the PCS has no waiting time and a shorter riding time because of the direct service without
 25 transfers. However, the PCS operation cost is higher than the MTNS operation cost by 290.86% due to
 26 the much lower vehicle occupancies in the PCS.

27 Based on Theorems 1 and 2, we obtain a lower bound objective $F_{LM}^* = 1457.91$ and an upper bound
 28 objective $F'_{NLM} = 1465.60$. This result yields an optimality gap of 0.52%, which is on a lower order of
 29 magnitude than the cost component improvements in Table 6 and consequently acceptable.

30 **Table 6 Cost comparisons of different operating systems (case 1)**

	MTNS		FSBS		PCS	
	Value	Value	% reduction	Value	% reduction	
• System cost	\$1,457.91	\$1,561.43	7.10%	\$1,880.17	28.96%	
Revised system cost*	\$329.81	\$433.33	31.39%	\$752.07	128.03%	
• Operation cost	\$192.41	\$257.11	33.63%	\$752.07	290.86%	
• Waiting time cost	\$135.34	\$144.23	6.57%	-	-	
• Riding time cost	\$1,128.47	\$1,135.81	0.65%	\$1,128.10	-0.03%	
Revised riding time cost*	\$0.37	\$7.71	1983.78%	-	-	
• Transfer cost	\$1.71	\$24.29	1316.67%	-	-	

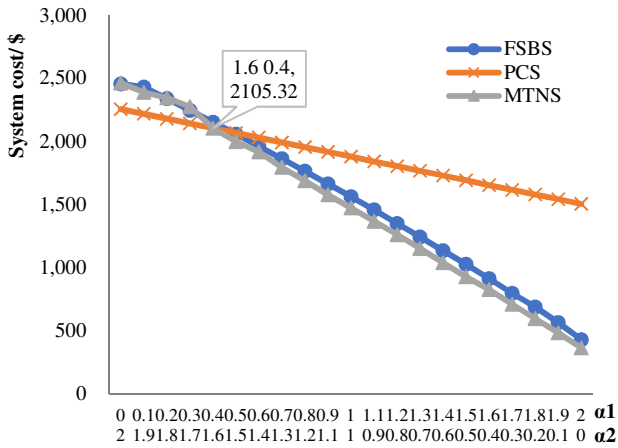
31 Note: The revised system cost and revised riding time cost are calculated by removing the fixed free-flow
 32 travel time (equal to the riding time cost in the PCS), which is independent of the optimal decisions.

33 *Sensitivity analysis*

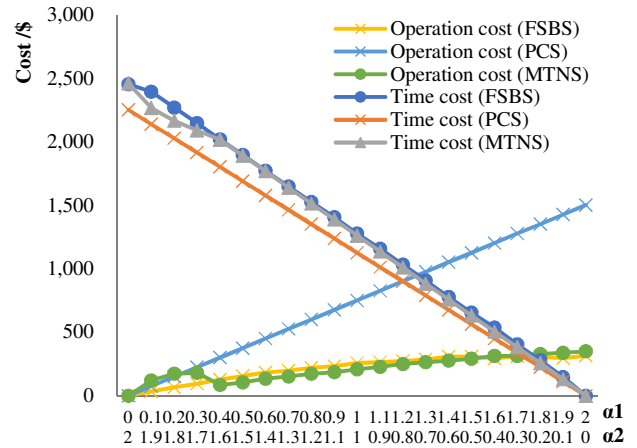
34 This section analyzes the sensitivity of cost components to critical parameters in all three systems.
 35 Only one parameter is varied in each instance, and the other parameters remain at their default values.
 36 To evaluate the performance for different cases, we compared the overall system cost, operation cost,

riding time cost, waiting time cost, and transfer cost. To simplify the sensitivity analysis for c_s and c_t , we introduced two rates to adjust the values as $c'_s = \alpha_1 * c_s$ and $c'_t = \alpha_2 * c_t$. Rates α_1 and α_2 are varied with $\alpha_1 + \alpha_2 = 2$, where $\alpha_1, \alpha_2 \in \mathbb{N}^+$. The results are plotted in Figure 5. The findings of parameters α_1, α_2, S , and β are briefly summarized as follows.

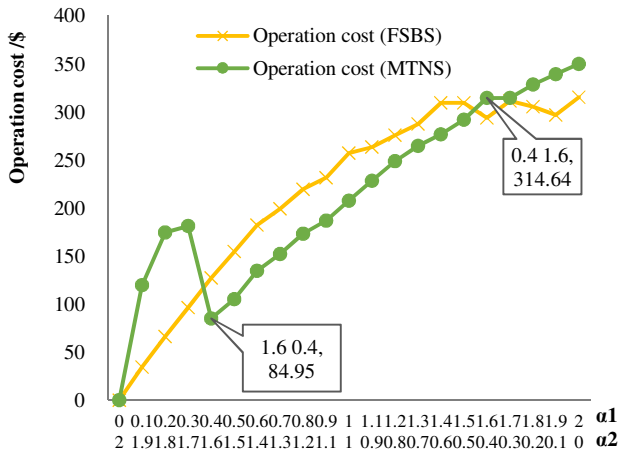
- Figure 5(a) and (b) show that the proposed MTNS model effectively reduces the system cost. Compared to the FSBS, the MTNS always performs better (e.g., with a lower system costs) at all α_1 and α_2 values. Figure 5(c) plots the operation cost with varying α_1 and α_2 values. The operation cost of the MTNS increases when the trip time cost dominates ($\alpha_1 \leq 0.4, \alpha_2 \geq 1.6$). Compared to the PCS, the system cost of the MTNS is lower when the operation cost rate is relatively high over the trip time cost range ($\alpha_1 \geq 0.4, \alpha_2 \leq 1.6$). However, when the time cost dominates ($\alpha_1 \leq 0.4, \alpha_2 \geq 1.6$), the PCS may work better than the MTNS due to its time savings from direct service.
- Figure 5(d) plots the transfer cost with varying α_1 and α_2 values. The transfer cost in the FSBS significantly increases with the increase in operation cost, while that of the MTNS does not vary much with changes in α_1 and α_2 .
- The system cost decreases when the number of MV types (or S) increases, as shown in Figure 5(e). This result is evident because more MV types provide more flexible vehicle capacities. The system cost in the FSBS is a U-shaped curve with an optimal value of $S = 6$ (i.e., $n^F = 36$), which is the default parameter value that we selected in the numerical example.
- Figure 5(f) shows the sensitivity of the system cost to transfer cost β . The system cost increases when the transfer cost rate per passenger increases. However, the transfer cost shares a small percentage of the system cost in the MTNS, and the magnitude of the increase in system cost is not substantial. The transfer cost per passenger increases by 900% (i.e., from 0.07 to 0.71), while the total system cost only increases by 0.3% (i.e., from \$1456 to \$1461).



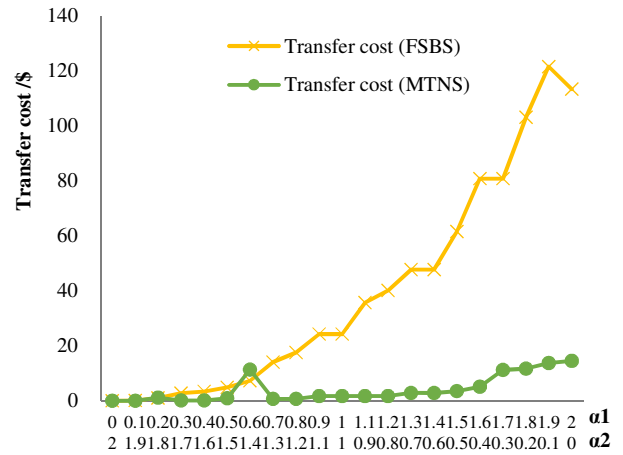
(a) System cost performance with α_1, α_2



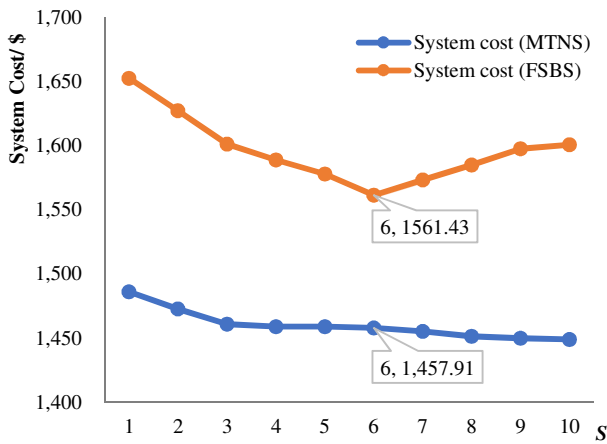
(b) Cost performance with α_1, α_2



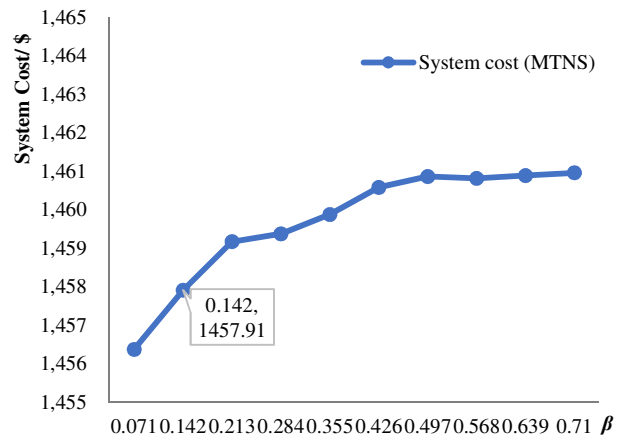
(c) Operation cost performance with α_1 and α_2



(d) Transfer cost performance with α_1 and α_2



(e) System cost performance with MV type S for the MTNS and n_F for the FSBS, $n^F = S * 6$



(f) System cost performance with transfer cost β

1 **Figure 5 Sensitivity analysis of the criterion with different input parameters**

2 The above obtained optimal solutions to the LM may not be the exact optima to the original NLM.
 3 To investigate the approximation errors, we employ Theorems 1 and 2 to quantify the corresponding
 4 approximation gaps for a set of selected instances with different parameter settings, as shown in Table 7.
 5 The approximation gaps are less than 4% for all instances with an average of 1.66%, which is acceptable
 6 for engineering practice. If we further refine the linearization approximation intervals, we expect the
 7 gaps to continue to decrease (although more computational resources are required).

8 **Table 7 Sensitivity analysis of the approximation gap with various parameter combinations**

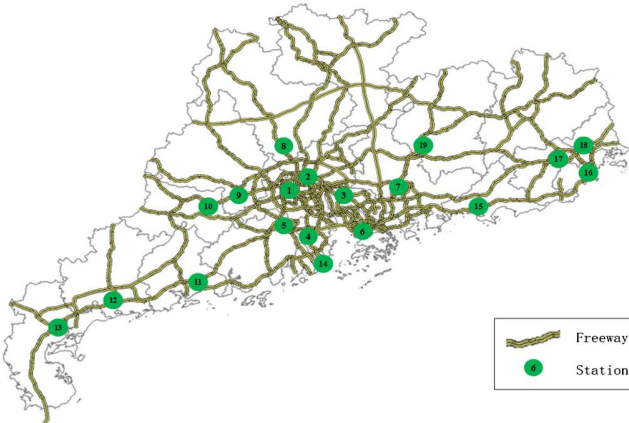
Instance number	α_1	α_2	S	β	F_{LM}^*	F'_{NLM}	Approximation gap
1	0	2	6	0.142	\$2,464.89	\$2,520.91	2.22%
2	0.5	1.5	6	0.142	\$2,000.41	\$2,054.86	2.65%
3	1	1	6	0.142	\$1,457.91	\$1,465.60	0.52%
4	1.5	0.5	6	0.142	\$928.03	\$957.41	3.07%
5	2	0	6	0.142	\$364.40	\$379.30	3.93%
6	1	1	2	0.142	\$1,472.78	\$1,483.56	0.73%
7	1	1	4	0.142	\$1,459.00	\$1,480.25	1.44%

8	1	1	8	0.142	\$1,451.39	\$1,464.36	0.89%
9	1	1	10	0.142	\$1,449.00	\$1,462.30	0.91%
10	1	1	6	0.071	\$1,456.38	\$1,475.15	1.27%
11	1	1	6	0.213	\$1,459.17	\$1,475.63	1.12%
12	1	1	6	0.284	\$1,459.38	\$1,475.74	1.11%
Average							1.66%

4.2 Nineteen-station example

To examine the model performance over different network topologies, we present another example with more stations (19 stations) and a larger network (the Guangdong Province freeway network). At this province-level spatial scale, the operations involve a new shared-mobility freeway system where travelers travel from one freeway station to another freeway station with shared MVs instead of driving their cars. For example, each traveler selects a urban transportation service (e.g., bus, metro, BRT, taxi, shared bike, or MV) from their origin (e.g., home or office) to the nearest shared MTNS freeway service station. Then, an MV transports the passenger to the MTNS freeway service station that is nearest to the passenger destination. Finally, from this service station, the passenger transfers to another urban transportation service to reach their destination. This study assumes that local transportation decisions are exogenous to MTNS decisions; thus, the local transportation costs are not considered. The advantages of this proposed new system are associated with pooling riders in MVs with high occupancy (as opposed to the low occupancy in the PCS) and flexible capacity (as opposed to the fixed capacity in the FSBS).

The input data include 295876 records of vehicles passing through 19 key toll stations in Guangdong, China (see Figure 6(a)), from 10:00-11:00 in May 2019. With an estimated average occupancy of 1.5 passengers per vehicle (Chow et al., 2010; Johnston and Ceerla, 1996; Siuhi and Mussa, 2007), we obtain the passenger OD demands as shown in Figure 6(b). We assume that 3% of the passengers use the MTNS service by default; we set $M = 20$, and $\tau = [0.1: 0.025: 0.45, 0.5, 1, 500, 1000]$.



	1	2	3	4	5	6	7	8	9	10	11	12	13	14	15	16	17	18	19
1	0	7355	4418	886	1487	1754	1406	2541	864	245	137	68	79	674	86	61	103	19	352
2	5825	0	855	1821	2190	395	208	181	2597	534	162	61	84	403	14	11	14	5	35
3	4490	933	0	270	632	827	1930	258	171	100	41	36	31	209	59	25	35	11	244
4	576	1808	197	0	1409	117	40	37	117	108	204	53	61	634	4	1	3	2	3
5	1392	1786	571	1423	0	313	89	13	65	83	75	28	39	1261	6	7	11	4	20
6	1850	437	5838	141	442	0	3317	82	85	52	19	33	13	199	191	46	87	14	284
7	1265	145	1595	42	66	2643	0	51	44	26	4	5	6	33	234	25	76	24	484
8	2047	159	241	18	10	71	53	0	107	14	7	2	2	14	3	1	0	2	10
9	674	2192	148	97	51	42	42	88	0	223	13	3	3	39	4	3	5	3	14
10	213	470	125	103	73	40	15	13	269	0	130	10	16	35	2	1	2	6	6
11	105	142	42	244	66	33	7	9	5	133	0	154	86	41	0	0	0	1	0
12	71	112	50	80	39	25	12	2	6	38	190	0	421	14	0	0	1	1	4
13	117	135	43	138	54	35	9	4	6	20	121	410	0	32	0	1	2	0	6
14	471	260	199	644	1169	176	35	10	52	31	61	21	17	0	11	1	5	2	8
15	107	4	50	3	8	222	253	5	3	2	1	1	7	4	0	36	149	20	6
16	60	11	26	1	5	59	42	3	4	2	0	1	0	6	49	0	1094	739	19
17	114	13	48	1	9	93	76	4	5	2	1	1	3	9	137	892	0	303	38
18	30	8	13	3	1	16	18	0	3	0	0	0	0	1	14	595	260	0	8
19	338	38	185	9	15	216	448	18	18	13	1	1	2	4	2	3	20	9	0

(a) 19 key toll stations in Guangdong Province, China

(b) OD demand data

Figure 6 Toll station information and OD demand data in Guangdong Province, China

In this case, the optimal results of the three systems are shown in Table 8. Compared to the FSBS, the MTNS performs well in reducing the system cost (by 4.62%). Again, this result is further improved (to 15.98%) when we omit the free-flow travel time cost, which is a constant component in this system. If we decompose the total system cost into different components, we see significant improvements in the critical cost components. Specifically, the operation cost and waiting time cost are reduced by 2.29% and 9.76%, respectively. This reduction indicates the advantages of the proposed MTNS over the

1 traditional FSBS. While the riding time cost does not dramatically change, it is dominated by the travel
2 distance (range of approximately 100-800 km in this case) and consequently not much affected by the
3 transportation system. If we remove the free-flow travel time cost, we see a much more significant
4 improvement in the variable riding time cost (by 111.67%). The passenger transfer cost is also optimized
5 in the MTNS. Compared to the PCS, the MTNS yields dramatic savings in operation cost and system
6 cost, but the time costs slightly increase due to the added waiting and transfers. Finally, the MTNS
7 model produces a lower bound $F_{LM}^* = 23,082.86$ and an upper bound $F'_{NLM} = 23,351.55$, which yield
8 an optimality gap of 1.15% with a computational time of 0.3 h.

9 **Table 8 Cost comparison of different operation systems (case 2)**

	MTNS		FSBS		PCS	
	Value	Value	% reduction	Value	% reduction	
• System cost	\$23,082.86	\$24,148.43	4.62%	\$49,026.99	112.40%	
• Revised system cost*	\$6,667.71	\$7,733.29	15.98%	\$32,611.84	389.10%	
• Operation cost	\$6,042.37	\$6,632.29	9.76%	\$32,611.84	439.72%	
• Waiting time cost	\$263.56	\$269.59	2.29%	-	-	
• Riding time cost	\$16,748.82	\$17,121.43	2.22%	\$16,415.14	-1.99%	
• Revised riding time cost*	\$333.68	\$706.29	111.67%	-	-	
• Transfer cost	\$28.10	\$125.13	345.27%	-	-	

10 Note: The revised system cost and revised riding time cost are calculated by removing the fixed free-flow
11 travel time (equal to the riding time cost of the PCS), which is independent of the optimal decisions.

12 5. Conclusion

13 Using the emerging MV technology, this paper proposes an approach to determine the optimal
14 MTNS design (i.e., the allocation and scheduling of MV fleets over a general transportation network) to
15 minimize the operation cost and passenger trip time cost. We formulate this problem into an MINLP
16 model that captures detailed traveler waiting time costs with nonlinear vehicle scheduling functions. To
17 facilitate the solution approach, we mathematically revise the MINLP model to produce a
18 computationally tractable mixed-integer linear programming (MILP) model. This linear model solves
19 both lower and upper bounds to the original nonlinear model and consequently yields a near-optimal
20 solution with an optimality gap. This revised MILP model can be solved by using off-the-shelf
21 commercial solvers (e.g., Gurobi) to obtain the exact solution. We explore two numerical examples to
22 illustrate the applications of this model and compare it with alternative systems (i.e., the FSBS and
23 PCS). The MTNS is more effective than the alternatives in suburban setting (reducing the system cost,
24 operation cost, and waiting time cost by 7.10%, 33.63%, and 6.57%, respectively, compared to the FSBS
25 and the operation cost and system cost by 290.86% and 28.96%, respectively, compared to the PCS) and
26 freeway settings (reducing the system cost and operation cost by 4.62% and 9.76% compared to the
27 FSBS and by 439.72% and 112.40% compared to the PCS, respectively). To further explore the
28 robustness of the proposed model with different input parameters, a sensitivity analysis shows the effects
29 of the crucial parameter values and approximation gaps on the MTNS performance.

30 Since the MV transit network system design is a novel research topic, the proposed model provides a
31 foundation that may be extended in several directions. The proposed model is formulated as a mixed-
32 integer linear programming problem and solved with a commercial solver (i.e., Gurobi) in this study.
33 Future work may focus on designing customized algorithms to further improve the solution efficiency.
34 Additional research is required to explore the dynamic and stochastic demands, en route link transfers,
35 and associated vehicle coordination when operating a mixed fleet on the link. The proposed model can
36 be extended to consider the intercedence among system design decisions, traffic congestion patterns, and
37 heterogeneous passenger behaviors (e.g., preferences regarding time windows, service level, willingness

1 to pay, and MV type). Moreover, it will be interesting to examine the effect of the combinations of
2 autonomous and electric MVs in future transportation modes.

3 **References**

- 4 Almasi, M.H., Sadollah, A., Oh, Y., Kim, D.K., Kang, S., 2018. Optimal coordination strategy for an integrated multimodal
5 transit feeder network design considering multiple objectives. *Sustain.* 10. <https://doi.org/10.3390/su10030734>
- 6 Alshalalfah, B., Shalaby, A., 2012. Feasibility of Flex-Route as a Feeder Transit Service to Rail Stations in the Suburbs: Case
7 Study in Toronto. *J. Urban Plan. Dev.* 138, 90–100. [https://doi.org/10.1061/\(ASCE\)UP.1943-5444.0000096](https://doi.org/10.1061/(ASCE)UP.1943-5444.0000096)
- 8 Ansari Esfeh, M., Wirasinghe, S.C., Saidi, S., Kattan, L., 2020. Waiting time and headway modelling for urban transit
9 systems—a critical review and proposed approach. *Transp. Rev.* 0, 1–23.
10 <https://doi.org/10.1080/01441647.2020.1806942>
- 11 Brown, D., Daganzo, C.F., 1992. *Logistics Systems Analysis.*, The Journal of the Operational Research Society. Springer.
12 <https://doi.org/10.2307/2584276>
- 13 Caros, N.S., Chow, J.Y.J., 2020. Day-to-day market evaluation of modular autonomous vehicle fleet operations with en-route
14 transfers. *Transp. B.* <https://doi.org/10.1080/21680566.2020.1809549>
- 15 Cepeda, M., Cominetti, R., Florian, M., 2006. A frequency-based assignment model for congested transit networks with strict
16 capacity constraints: Characterization and computation of equilibria. *Transp. Res. Part B Methodol.* 40, 437–459.
17 <https://doi.org/10.1016/j.trb.2005.05.006>
- 18 Chen, Z., Li, X., Zhou, X., 2020. Operational design for shuttle systems with modular vehicles under oversaturated traffic:
19 Continuous modeling method. *Transp. Res. Part B Methodol.* 132, 76–100. <https://doi.org/10.1016/j.trb.2019.05.018>
- 20 Chen, Z., Li, X., Zhou, X., 2019. Operational design for shuttle systems with modular vehicles under oversaturated traffic:
21 Discrete modeling method. *Transp. Res. Part B Methodol.* 122, 1–19. <https://doi.org/10.1016/J.TRB.2019.01.015>
- 22 Chow, J.Y.J., Lee, G., Yang, I., 2010. Genetic Algorithm to Estimate Cumulative Prospect Theory Parameters for Selection
23 of High-Occupancy-Vehicle Lane. *Transp. Res. Rec. J. Transp. Res. Board* 71–77. <https://doi.org/10.3141/2157-09>
- 24 Cochran, J.J., Cox, L.A., Keskinocak, P., Kharoufeh, J.P., Smith, J.C., Linderoth, J.T., Lodi, A., 2011. MILP Software, in:
25 *Wiley Encyclopedia of Operations Research and Management Science.* John Wiley & Sons, Inc.
26 <https://doi.org/10.1002/9780470400531.eorms0524>
- 27 Daganzo, C.F., 2010. Structure of competitive transit networks. *Transp. Res. Part B Methodol.* 44, 434–446.
28 <https://doi.org/10.1016/j.trb.2009.11.001>
- 29 Dai, Z., Liu, X.C., Chen, X., Ma, X., 2020. Joint optimization of scheduling and capacity for mixed traffic with autonomous
30 and human-driven buses: A dynamic programming approach. *Transp. Res. Part C Emerg. Technol.* 114, 598–619.
31 <https://doi.org/10.1016/j.trc.2020.03.001>
- 32 Diana, M., Dessouky, M.M., Xia, N., 2006. A model for the fleet sizing of demand responsive transportation services with
33 time windows. *Transp. Res. Part B Methodol.* 40, 651–666. <https://doi.org/10.1016/j.trb.2005.09.005>
- 34 Fan, W., Mei, Y., Gu, W., 2018. Optimal design of intersecting bimodal transit networks in a grid city. *Transp. Res. Part B*
35 *Methodol.* 111, 203–226. <https://doi.org/10.1016/j.trb.2018.03.007>
- 36 Fuentes, M., Cadarso, L., Marín, Á., 2019. A hybrid model for crew scheduling in rail rapid transit networks. *Transp. Res.*
37 *Part B Methodol.* 125, 248–265. <https://doi.org/10.1016/j.trb.2019.05.007>
- 38 Gorski, J., Pfeuffer, F., Klamroth, K., 2007. Biconvex sets and optimization with biconvex functions: A survey and
39 extensions. *Math. Methods Oper. Res.* 66, 373–407. <https://doi.org/10.1007/s00186-007-0161-1>
- 40 Guo, Q.W., Chow, J.Y.J., Schonfeld, P., 2018. Stochastic dynamic switching in fixed and flexible transit services as market
41 entry-exit real options. *Transp. Res. Part C Emerg. Technol.* 94, 288–306. <https://doi.org/10.1016/j.trc.2017.08.008>
- 42 Guo, X., Sun, H., Wu, J., Jin, J., Zhou, J., Gao, Z., 2017. Multiperiod-based timetable optimization for metro transit networks.
43 *Transp. Res. Part B Methodol.* 96, 46–67. <https://doi.org/10.1016/j.trb.2016.11.005>
- 44 Johnston, R.A., Ceerla, R., 1996. The effects of new high-occupancy vehicle lanes on travel and emissions. *Transp. Res. Part*
45 *A Policy Pract.* 30, 35–50. [https://doi.org/10.1016/0965-8564\(95\)00009-7](https://doi.org/10.1016/0965-8564(95)00009-7)
- 46 Liberti, L., Pantelides, C.C., 2006. An exact reformulation algorithm for large nonconvex NLPs involving bilinear terms. *J.*
47 *Glob. Optim.* 36, 161–189. <https://doi.org/10.1007/s10898-006-9005-4>
- 48 Liu, T., (Avi) Ceder, A., 2017. Deficit function related to public transport: 50 year retrospective, new developments, and
49 prospects. *Transp. Res. Part B Methodol.* 100, 1–19. <https://doi.org/10.1016/j.trb.2017.01.015>
- 50 Nassir, N., Hickman, M., Malekzadeh, A., Irannezhad, E., 2016. A utility-based travel impedance measure for public transit
51 network accessibility. *Transp. Res. Part A Policy Pract.* 88, 26–39. <https://doi.org/10.1016/j.tra.2016.03.007>
- 52 NextFutureTransport [WWW Document], n.d. URL <https://www.next-future-mobility.com/> (accessed 7.27.19).
- 53 Niu, H., Zhou, X., Gao, R., 2015. Train scheduling for minimizing passenger waiting time with time-dependent demand and
54 skip-stop patterns: Nonlinear integer programming models with linear constraints. *Transp. Res. Part B Methodol.* 76,

1 117–135. <https://doi.org/10.1016/j.trb.2015.03.004>

2 Nourbakhsh, S.M., Ouyang, Y., 2012. A structured flexible transit system for low demand areas. *Transp. Res. Part B*

3 *Methodol.* 46, 204–216. <https://doi.org/10.1016/j.trb.2011.07.014>

4 Ohmio [WWW Document], n.d. URL <https://ohmio.com/> (accessed 7.27.19).

5 Ortega, F., Wolsey, L.A., 2003. A Branch-and-Cut Algorithm for the Single-Commodity, Uncapacitated, Fixed-Charge

6 Network Flow Problem. *Networks* 41, 143–158. <https://doi.org/10.1002/net.10068>

7 Ouyang, Y., Nourbakhsh, S.M., Cassidy, M.J., 2014. Continuum approximation approach to bus network design under

8 spatially heterogeneous demand. *Transp. Res. Part B Methodol.* 68, 333–344. <https://doi.org/10.1016/j.trb.2014.05.018>

9 Owen, A., Levinson, D.M., 2015. Modeling the commute mode share of transit using continuous accessibility to jobs. *Transp.*

10 *Res. Part A Policy Pract.* 74, 110–122. <https://doi.org/10.1016/j.tra.2015.02.002>

11 Pei, M., Lin, P., Liu, R., Ma, Y., 2019a. Flexible transit routing model considering passengers' willingness to pay. *IET Intell.*

12 *Transp. Syst.* 13, 841–850. <https://doi.org/10.1049/iet-its.2018.5220>

13 Pei, M., Lin, P., Ou, J., 2019b. Real-Time Optimal Scheduling Model for Transit System with Flexible Bus Line. *Transp. Res.*

14 *Rec. J. Transp. Res. Board* 2673, 036119811983750. <https://doi.org/10.1177/0361198119837502>

15 Quadrifoglio, L., Dessouky, M.M., Ordóñez, F., 2008. A simulation study of demand responsive transit system design.

16 *Transp. Res. Part A Policy Pract.* 42, 718–737. <https://doi.org/10.1016/j.tra.2008.01.018>

17 Quadrifoglio, L., Dessouky, M.M., Palmer, K., 2007. An insertion heuristic for scheduling Mobility Allowance Shuttle

18 Transit (MAST) services. *J. Sched.* 10, 25–40. <https://doi.org/10.1007/s10951-006-0324-6>

19 Quadrifoglio, L., Hall, R.W., Dessouky, M.M., 2006. Performance and Design of Mobility Allowance Shuttle Transit

20 Services: Bounds on the Maximum Longitudinal Velocity. *Transp. Sci.* 40, 351–363.

21 <https://doi.org/10.1287/trsc.1050.0137>

22 Rau, A., Tian, L., Jain, M., Xie, M., Liu, T., Zhou, Y., 2019. Dynamic Autonomous Road Transit (DART) for Use-case

23 Capacity More Than Bus. *Transp. Res. Procedia* 41, 812–823. <https://doi.org/10.1016/j.trpro.2019.09.131>

24 Sayarshad, H.R., Chow, J.Y.J., 2015. A scalable non-myopic dynamic dial-a-ride and pricing problem. *Transp. Res. Part B*

25 *Methodol.* 81, 539–554. <https://doi.org/10.1016/j.trb.2015.06.008>

26 Shi, X., Chen, Z., Pei, M., Li, X., 2020. Variable-Capacity Operations with Modular Transits for Shared-Use Corridors.

27 *Transp. Res. Rec. J. Transp. Res. Board.*

28 Siuhi, S., Mussa, R., 2007. Simulation analysis of truck-restricted and high-occupancy vehicle lanes. *Transp. Res. Rec.* 127–

29 133. <https://doi.org/10.3141/2012-15>

30 Tong, C.O., Wong, S.C., 1999. Schedule-based time-dependent trip assignment model for transit networks. *J. Adv. Transp.*

31 33, 371–388. <https://doi.org/10.1002/atr.5670330307>

32 Tong, L., Zhou, X., Miller, H.J., 2015. Transportation network design for maximizing space-time accessibility. *Transp. Res.*

33 *Part B Methodol.* 81, 555–576. <https://doi.org/10.1016/j.trb.2015.08.002>

34 Wang, S., Qu, X., 2015. Rural bus route design problem: Model development and case studies. *KSCE J. Civ. Eng.* 19, 1892–

35 1896. <https://doi.org/10.1007/s12205-013-0579-3>

36 Wu, W., Liu, R., Jin, W., 2016. Designing robust schedule coordination scheme for transit networks with safety control

37 margins. *Transp. Res. Part B Methodol.* 93, 495–519. <https://doi.org/10.1016/j.trb.2016.07.009>

38 Zhang, Y., D'Ariano, A., He, B., Peng, Q., 2019. Microscopic optimization model and algorithm for integrating train

39 timetabling and track maintenance task scheduling. *Transp. Res. Part B Methodol.* 127, 237–278.

40 <https://doi.org/10.1016/j.trb.2019.07.010>

41 Zhang, Z., Tafreshian, A., Masoud, N., 2020. Modular transit: Using autonomy and modularity to improve performance in

42 public transportation. *Transp. Res. Part E Logist. Transp. Rev.* 141, 102033. <https://doi.org/10.1016/j.tre.2020.102033>

43